JOINT INSTITUTE FOR NUCLEAR RESEARCH
Veksler and Baldin laboratory of High Energy Physics

FINAL REPORT ON THE SUMMER STUDENT PROGRAM

Studies of femtoscopy correlations within the NICA energy range

Supervisors:
Oleg Rogachevsky
Ludmila Malinina
Pavel Batyuk

Author:
Maria Stefaniak, Poland
Warsaw University of Technology

Participation period:
27.07 - 02.09.2016

Dubna, 2016

1 Abstract

Collisions of heavy-ions are major method used to study properties of matter. In order to examine such tiny objects, the special conditions must be guaranteed. So that in huge laboratories the beams of ions are prepared, accelerated and collided. The most precise technology is used to detect newly created matter and collect the information on it.

The construction of new experiments is a crucial task in development of science. It increases the variety of possible measurements and allows one to create different conditions to study the physics of created system. One of such experiments is now under construction in Dubna (Russia). The project called NICA[1] is run at Joint Institute for Nuclear Research (JINR). As all of technical devices, the detectors in Dubna also will have some limitations like time and space resolution or speed of data transfer. The significant one is to make some predictions on possible results to be obtained within experiments on the NICA facility. Different Monte-Carlo generators are used with a goal to perform simulations of heavy-ions collisions in the same conditions as in the experiment. It allows one to perform different kinds of analysis and arrive at a conclusion what influence on collecting data is made by those limitations.

One of the basic tools in process of analysis are studies of femtoscopy correlations. It allows one to measure size and shape of source determined by newly created particles. The program which calculates such correlation will be created. The analysis will be performed for data simulated by the vHLLE + UrQMD hybrid model.

[1]Nuclotron-based Ion Collider Facility

2 NICA experiment

NICA is a crucial project to be run at JINR. Already existing in the Institute accelerating complex will be used as a part of NICA. Primary acceleration (BOOSTER) will be performed in the ring, where there used to be a synchrophasotron built in 1957. Now there is located *NUCLOTRON*, which is already in operation. The last acceleration step will be in the NICA collider. The project will consists of three experimental sub-complexes:

- BM@N[2] - extracted ion beams accelerated in Nuclotron are collided in a fix-target experiment[3]. In 2017 the BM@N is planned to be put in operation completely.
- MPD[4] - two beams are accelerated in opposite directions and collided inside the MPD detector. The variety of future performed kinds of analysis requires high standards of measurements (high level of luminosity and resolution). In 2019 the MPD is planned to be put in operation (the first stage of the experiment).
- SPD[5] - collisions are obtained similarly to the MPD. The experiment will focus on studies of possible spin effects.

A current structure of the NICA complex is shown in Fig. 1.

The main motivation of the NICA project is an exploration of the QCD[6] phase diagram in area of moderate temperatures and high values of baryon densities [1].

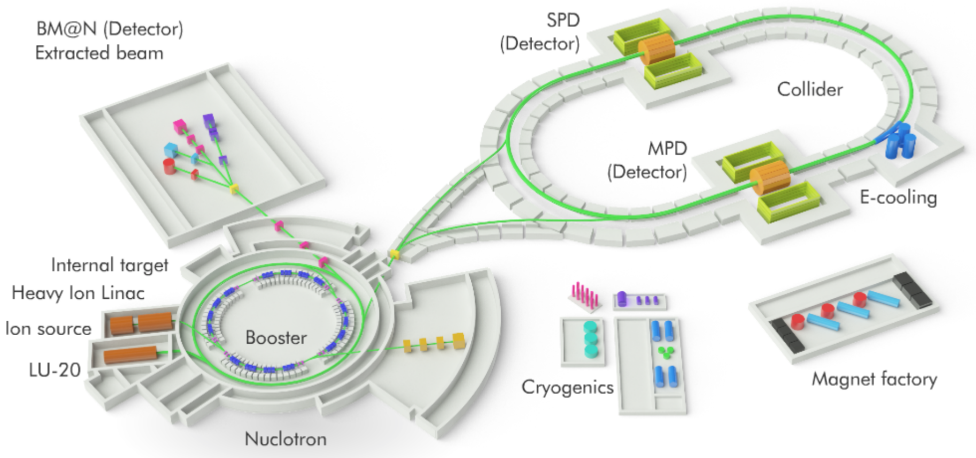

Figure 1: The NICA complex at JINR [2].

[2]Baryonic Matter at Nuclotron
[3]An experiment where the accelerated beam hits a static target
[4]Multi-Purpose Detector
[5]Spin Physics Detector
[6]Quantum Chromodynamic

2.1 NICA and the QCD Phase Diagram

The properties of matter at high temperatures and densities can be studied in special conditions. According to the QCD calculations the transition between hadron gas and quark-gluon plasma is possible to occur in systems created after ion collisions in the NICA energy range ($\sqrt{S_{NN}}$ = 4 - 11 GeV). When the matter achieves thermodynamic stability the partons[7] are not bounded into hadrons and mesons anymore, they prosper as single particles. This state is called quark-gluon plasma. The QCD phase diagram illustrates the dependence of the state of the matter on the conditions such as temperature T and chemical barionic potential μ_B. In Fig. 2 are shown the areas on QCD phase diagram which are possible to explore with such experimental complexes as STAR[8], NICA and Nuclotron-M.

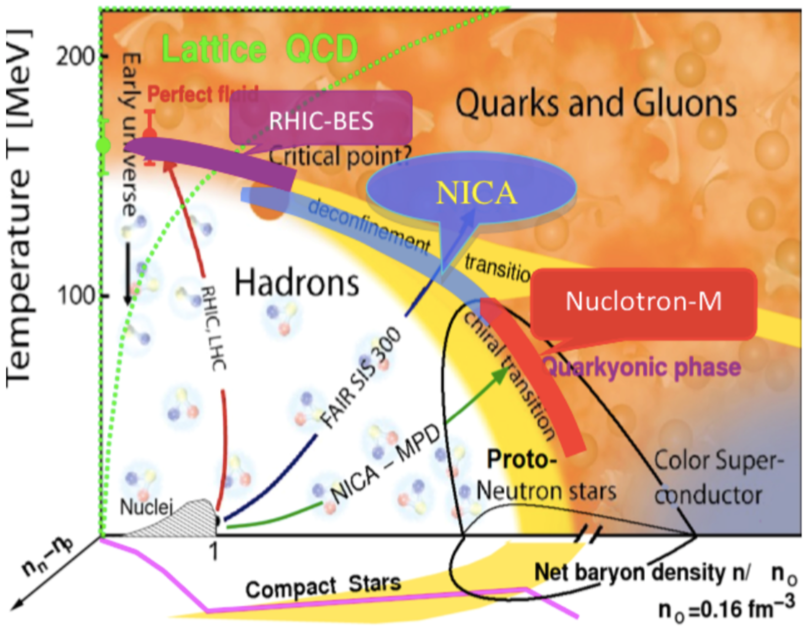

Figure 2: Quantum Chromodynamic Phase Diagram [1]

One of the tools used in examining the QCD phase diagram are studies of femtoscopy correlations, described in the next section.

[7]quarks, gluons

[8]Solenoid Tracker At RHIC

3 Femtoscopy correlations

"Originally correlations method was performed in astronomy. Investigation of electromagnetic signals measured in coincidence allowed one to find parameters describing stellar objects' sizes. Authors R. Hanbury-Brown and R. Q. Twiss did not know about nowadays application of their measurement method. It was transformed in order to focus on the smallest sizes in nature, about $10^{-15}m$. In this range, in Particle Physics, these method is called "femtoscopy". Two-particle correlations use particles' momenta and make it possible to examine space-time extent of the emitting source created during the collisions of nuclei.

3.0.1 Correlation function

A two-particle correlation function defines ratio between probability of detecting two particles with given momenta and position simultaneously to product of detecting them separately.

$$C(p_1, p2) = \frac{P_2(p_1, p_2)}{P_1(p_1)P_1(p_2)} \tag{1}$$

where:

$$P_2(p_1, p_2) = E_1 E_2 \frac{dN}{d^3 p_1 p_2} = \int d^4x_1 S(x_1, p_1) d^4x_2 S(x_2, p_2) \Phi(x_2, p_2 | x_1, p_1) \tag{2}$$

$$P_1(p) = E \frac{dN}{d^3 p} = \int d^4 x S(x, p) \tag{3}$$

where

$S(x, p)$ is an emission function: the distribution of the source density probability of detecting a particle with x and p.

The source is often treated as a three-dimensional sphere. Kopylov and Podgoretsky proposed a parametrization of this object using a three-vector **q**, defining the momentum difference between particles in a considering pair, and a constant λ [3], where:

$$\vec{q} = \vec{p_1} - \vec{p_2} \tag{4}$$

The momentum difference is expanded over q_{long}, q_{out} and q_{side}, where the "long" axis goes along the beam, "out" - along the pair transverse momentum and "side" is perpendicular to the latter one in the transverse plane. In Fig. 3 a schematic view of the expansion is shown. Admitting this parametrization one can consider the correlation function to be represented in the following form:

$$C(q_{out}, q_{side}, q_{long}, \lambda) = 1 + \lambda exp(-q_{out}^2 r_{out}^2 - q_{side}^2 r_{side}^2 - q_{long}^2 r_{long}^2) \tag{5}$$

where $r_{out,side,long}$ are lengths of the source in *out*, *side* and *long* directions (three-dimensional femtoscopy radii) and λ is a strength of correlation.

The parametrization is a three-dimensional one since it allows one to extract the source shape in three separated directions. The calculations are performed in the LCMS[9] frame [3]. A representation of the correlation function giving an averaged Gaussian radius of the source is also possible and looks as follows:

$$C(Q_{inv}; r_0, \lambda) = 1 + \lambda exp(-Q_{inv}^2 R_0^2) \tag{6}$$

where R_0 is an averaged Gaussian radius of source, Q_{inv} is a relative momentum in the pair rest frame (PRF).

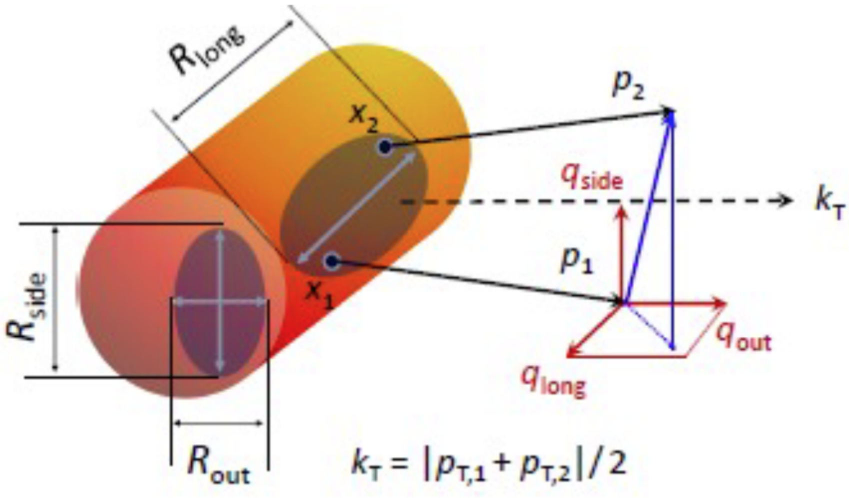

Figure 3: Definition the three-dimensional femtoscopy radii.

Dealing with experimental data one has to parametrize the two-particle correlation function with equation:

$$C_2(\vec{q}) = \frac{A(\vec{q})}{B(\vec{q})} \tag{7}$$

where A (signal) is a momentum distribution of particles built in the same event, while B (background) is a reference momentum distribution obtained from different events.

3.1 Shape of function

The shape of the correlation function depends on several phenomena. Fig. 4 shows two-particle correlation functions for protons obtained at including different physics effects (QS, QS + COUL,

[9] Longitudinal Co-Moving System

QS + COUL + SI, see below).

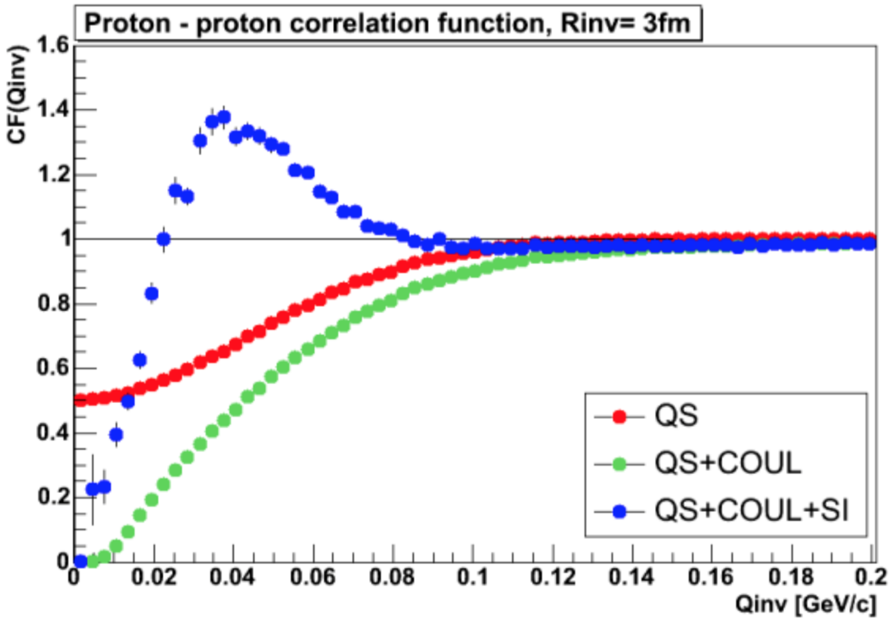

Figure 4: Proton - proton correlation functions assuming the source size equal to 3 fm [3].

The presented correlation functions can be divided into two groups:

1) Quantum Statistics (QS)- it could be observed in correlations of identical particles:

- baryons - the Bose-Einstein statistics
- fermions - the Fermi-Dirac statistics

In the first case the correlation is positive. However, fermions are limited by Pauli Exclusion Principle, so that the correlation is negative.The red colored curve represents the QS-influence on the shape on the correlation function. For $Q_{inv} = 0GeV$ it is equal to 0.5, so the correlation is negative.

2) Final State Interaction (FSI):

- Coulomb interaction
- strong interaction

The Coulomb interaction (Fig. 4 - green dots) depends on charge of the particle. In case of opposite-sign particles they attract each other, while repulsing otherwise. Consequently, this kind of interactions could be positive (opposite-sign particles) or negative (same-sign particles).

Strong interactions (SI) have a positive influence on shape of the correlation function (Fig. 4 - blue dots). In case of pion-pion correlations, the impact of SI is not sufficient. The most relevant are the Bose-Einstein statistics and the Coulomb interactions.

3.2 Detector effects

In experimental data, besides the QS and FSI, there are also other effects caused by limitations of a particle identification (PID) procedure, such as:

- merging - Two tracks that are spatially very close are falsely reconstructed as one. This will show up as an inefficiency of closed pairs compared to a sample of unaffected pairs.
- splitting - One track is falsely reconstructed as two tracks (or more). This will show up as an enhancement of closed pairs compared to an uncorrelated sample. These effects are very crucial while performing a correlation analysis since they could affect sufficiently the obtained correlation function leading to an incorrect estimation of source size.

3.3 Source size

Two-particle femtoscopy correlations are one of the elementary techniques to examine properties of the matter created in heavy-ion collisions [3].

3.3.1 One-dimensional correlation function

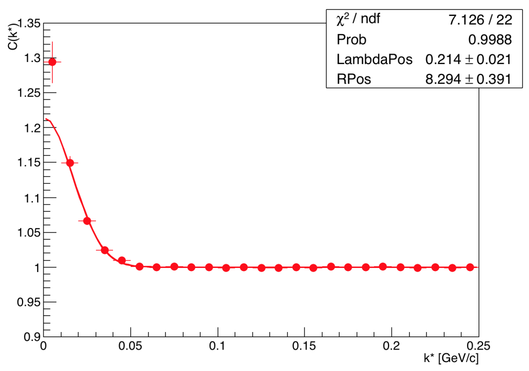

(a) Example of one-dimensional correlation function.

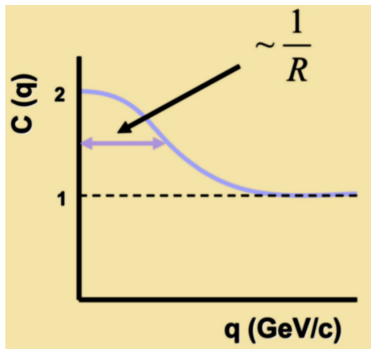

(b) Dependence of the source size on shape of the correlation function [4]

In case of an one-dimensional correlation analysis the shape of the source is assumed to be a sphere. Fig. 5b illustrates a dependence of the source size on shape of the correlation function.

3.3.2 Three-dimensional correlation function

In case of a three-dimensional analysis the out-direction width of the correlation function is inversely proportional to the lifetime of source (duration of particle emission). On the other hand, the side-direction measurements are inverse to the transverse size of source. However, the R_{side} and R_{out} are only proportional to the system average size or lifetime. Meanwhile measurements of radii are affected by hydrodynamical flow or it depends on the chosen reference frame. In order to make such effects more irrelevant or even cancel them out, one can study the ratio R_{out}/R_{side}. The system size is approximately constant, while the lifetime of source varies depending on presense of a phase transition. Hence, the R_{out}/R_{side} is considered to be optimal in studies of the lifetime of the system [5]." *fragment of Master thesis [6]*

4 Data Analysis

4.1 Data sample

In this research a correlation analysis dealing with positive charged pions producing in Au+Au collisions @ $\sqrt{s_{NN}} = 11.5 GeV$ has been performed. Approximately 100 000 events obtained from the vHLLE+UrQMD[**?**] hybrid model have been used.

4.2 Analysis software

The analysis has been performed within the FEMTOMPD package which is a part of the common software being used in the MPD experiment. Some crucial updates and optimizations have been introduced to the FEMTOMPD package during my internship.

4.3 Event and track selection

Criteria to be applied to the event are as follows:

- centrality of collision 0 - 5%
- each event has, at least, one pair of positively charged reconstructed and identified pions contributing to the signal distribution (nominator).

Criteria to be applied to the track selection are as follows:

- kinetic range for π^+: $\eta \in \{-1, 1\}$
- 10 events are used to construct a reference distribution (denominator)
- minimum value of hits per track is equal to 40
- considered pairs do not have common hits (sharing cut applied).

5 Results

5.1 Three-dimensional femtoscopy correlations

As mentioned, the FEMTOMPD package has been used for the analysis. Since it could perform an one-dimesional correlation analysis, a part responsible for the three dimensional analysis had to be created. Based on the one-dimensional one, a three-dimensional code, written in C++, which allows one to infer the size of emitting source, has been created. One of the most crucial points in the three-dimensional analysis is a definition of ranges of particle pair momentum k_T calculated as follows:

$$k_T = \frac{|p_{T,1} + p_{T,2}|}{2} \tag{8}$$

It gives an information on examined area of interacting particles.

An example of class previously created and used subsequently for definition and storing the output histograms related to the three-dimensional analysis, is shown in Fig. 6.

```
// Histos for 3D-analysis
const Int_t nBins3D = 60;
_hCFNom3D = new TH3D*[fKtBins];
_hCFDenom3D = new TH3D*[fKtBins];
_hCF3D = new TH3D*[fKtBins];
_XProjectNom  = new TH1D*[fKtBins];
_XProjectDenom = new TH1D*[fKtBins];
_XProject3D= new TH1D*[fKtBins];
_YProjectNom  = new TH1D*[fKtBins];
_YProjectDenom = new TH1D*[fKtBins];
_YProject3D= new TH1D*[fKtBins];
_ZProjectNom  = new TH1D*[fKtBins];
_ZProjectDenom = new TH1D*[fKtBins];
_ZProject3D= new TH1D*[fKtBins];

for (Int_t iKt = 0; iKt < fKtBins; iKt++) {
    _hCFNom3D[iKt] = new TH3D(Form("_kt%d_Nom_3D", iKt), Form("_kt%d_Nom_3D", iKt), nBins3D, 0., qInv, nBins3D, 0., qInv, nBins3D, 0., qInv);
    _hCFDenom3D[iKt] = new TH3D(Form("_kt%d_Denom_3D", iKt), Form("_kt%d_Denom_3D", iKt), nBins3D, 0., qInv, nBins3D, 0., qInv, nBins3D, 0., qInv);
    _hCF3D[iKt] = new TH3D(Form("_kt%d_CF_3D", iKt), Form("_kt%d_CF_3D", iKt), nBins3D, 0., qInv, nBins3D, 0., qInv, nBins3D, 0., qInv);
    _hCFNom3D[iKt]->Sumw2();
    _hCFDenom3D[iKt]->Sumw2();

    _XProjectNom[iKt] = new TH1D(Form("_kt%d_XProjNom_3D", iKt), Form("_kt%d_XProjNom_3D", iKt), nBins3D, 0., qInv);
    _XProjectDenom[iKt] = new TH1D(Form("_kt%d_XProjDenom_3D", iKt), Form("_kt%d_XProjDenom_3D", iKt), nBins3D, 0., qInv);
    _XProject3D[iKt] = new TH1D(Form("_kt%d_XProjCF_3D", iKt), Form("_kt%d_XProjCF_3D", iKt), nBins3D, 0., qInv);
    _YProjectNom[iKt] = new TH1D(Form("_kt%d_YProjNom_3D", iKt), Form("_kt%d_YProjNom_3D", iKt), nBins3D, 0., qInv);
    _YProjectDenom[iKt] = new TH1D(Form("_kt%d_YProjDenom_3D", iKt), Form("_kt%d_YProjDenom_3D", iKt), nBins3D, 0., qInv);
    _YProject3D[iKt] = new TH1D(Form("_kt%d_YProjCF_3D", iKt), Form("_kt%d_YProjCF_3D", iKt), nBins3D, 0., qInv);
    _ZProjectNom[iKt] = new TH1D(Form("_kt%d_ZProjNom_3D", iKt), Form("_kt%d_ZProjNom_3D", iKt), nBins3D, 0., qInv);
    _ZProjectDenom[iKt] = new TH1D(Form("_kt%d_ZProjDenom_3D", iKt), Form("_kt%d_ZProjDenom_3D", iKt), nBins3D, 0., qInv);
    _ZProject3D[iKt] = new TH1D(Form("_kt%d_ZProjCF_3D", iKt), Form("_kt%d_ZProjCF_3D", iKt), nBins3D, 0., qInv);
}

_R_out_kT_3D = new TGraph();
_R_side_kT_3D = new TGraph();
_R_long_kT_3D = new TGraph();
```

Figure 6: Definition of created histograms.

where:

$\_hCFNom3D$ is a nominator of the correlation function

$\_hCFDenom3D$ is a denominator of the correlation function

$\_hCF3D$ - is a correlation function

$\_(X/Y/Z)ProjectNom$ is a projection of the nominator of on X / Y / Z-axis

$\_(X/Y/Z)ProjectDenom$ is a projection of the denominator on X / Y / Z-axis

$\_(X/Y/Z)Project3D$ is a projection of the correlation function on X / Y / Z-axis

$\_R\_(out/side/long)\_kT\_3D$ are graphs with the calculated femtoscopy radii out / side / long directions

All the created histograms take into account affiliation to different k_T bins used being set in the main macro called *femtoAna.C* (see Fig. 7).

```
Int_t nKtBins = 4; //Define number of kT-bins to be used
const Int_t dim = nKtBins + 1;
Float_t KtRanges[dim] = {0.0, 0.2, 0.4, 0.6, 1}; //Define ranges of kT-bins
```

Figure 7: Setting the number and ranges of k_T bins.

The first part of the calculations is a correct definition of the mixing procedure. Those pairs of particles come from the same event are put into the nominator, while the denominator is filled by pairs of particles from different events. The procedure is shown in Figure 8.

```
for (Int_t iKt = 0; iKt < fHisto->GetfKtBins(); iKt++) {
    if (kt > fHisto->GetfKtRange(iKt) && kt < fHisto->GetfKtRange(iKt + 1)) {
        if (iPart_evNum == jPart_evNum) {
            fHisto->GetNominator3D(iKt)->Fill(q_out, q_side, q_long, wfemto);
            n++;
        }
        else {
            fHisto->GetDenominator3D(iKt)->Fill(q_out, q_side, q_long);
            d++;
        }
        break;
    }
}
```

Figure 8: An example of realization of the mixing procedure in the FEMTOMPD.

According to the definition, a result of devision of the nominator by the denominator is a two-correlation function to be obtained. The fitting procedure with the equation [5] is used (see Fig. 9) allowing one to extract values of the femtoscopy radii on out, side and long directions.

In order to verify the results it is possible to make projections of three-dimensional correlation function on X, Y and Z axis [Figure 10].

```
for (Int_t iKt = 0; iKt < fKtBins; iKt++) {
    TF3* fitc = new TF3("fitc", "1 + [3] * exp(-25.76578 * (x * x * [0] * [0] + y * y * [1] * [1] + z * z * [2] * [2]))");
    fitc->SetParLimits(3, 0.0, 1.0);
      fitc->SetParLimits(0, 0.0, 100.0);
      fitc->SetParLimits(1, 0.0, 100.0);
      fitc->SetParLimits(2, 0.0, 100.0);
      fitc->SetParameter(3, 0.1);
      fitc->SetParameter(0, 5.0);
      fitc->SetParameter(1, 5.0);
      fitc->SetParameter(2, 5.0);
    _hCF3D[iKt]->Fit(fitc, "SRQ", " ", 0., fQinv);
    Double_t* params = fitc->GetParameters();
    Rside.push_back(params[0]);
    Rout.push_back(params[1]);
    Rlong.push_back(params[2]);
    delete fitc;
}
```

Figure 9: Fitting procedure.

```
for (Int_t iKt = 0; iKt < fKtBins; iKt++) {

    _hCFNom3D[iKt]->GetXaxis()->SetRange(1,nBins3D);
    _hCFNom3D[iKt]->GetYaxis()->SetRange(1,1+wbin);
    _hCFNom3D[iKt]->GetZaxis()->SetRange(1,1+wbin);

    _hCFDenom3D[iKt]->GetXaxis()->SetRange(1,nBins3D);
    _hCFDenom3D[iKt]->GetYaxis()->SetRange(1,1+wbin);
    _hCFDenom3D[iKt]->GetZaxis()->SetRange(1,1+wbin);

    _XProjectNom[iKt] = (TH1D *)_hCFNom3D[iKt]->Project3D("xe");
    _XProjectDenom[iKt] = (TH1D *)_hCFDenom3D[iKt]->Project3D("xe");

    _XProjectNom[iKt]->Sumw2();
    _XProjectDenom[iKt]->Sumw2();

    _XProject3D[iKt]->Divide(_XProjectNom[iKt], _XProjectDenom[iKt], 1., 1., "B");
}
```

Figure 10: Creating projections of three-dimensional correlation function on X, Y and Z axis.

5.2 Projections

The calculated correlation functions have been projected on X, Y and Z axis with a goal to obtain one-dimensional correlation functions depending on q_{out}, q_{side} and q_{long}, respectively. The calculations have been performed for two k_T bins: [0.2 - 0.3] GeV/c and [0.3 - 0.4] GeV/c. The obtained results are presented in Fig. 11 and Fig. 12, respectively.

The results give the information on effects having influence on their shape. The Bose-Einstein enhancement is visible for low q values. This shape is a characteristic one for correlations functions obtained with identical pions. With the increase of the difference of particles' momentum the values of function become more constant. These obtained shapes of functions are in the range of expectations. However, there are some visible effects to be mentioned.

First of all, in all figures there is a visible negative peak for $q \approx 0$ (one point). It is a result of possible merging of the reconstructed tracks. In projection of q_{out} for $k_T \in [0.2 - 0.3]$ GeV/c (Fig. 11) values of the correlation function are increased with q_{out}. This fact could be explained with the effect called Long Range Correlations [7]. The momentum conservation law is preserved in case of real events (signal distribution, nominator), while violating for the mixed ones (background

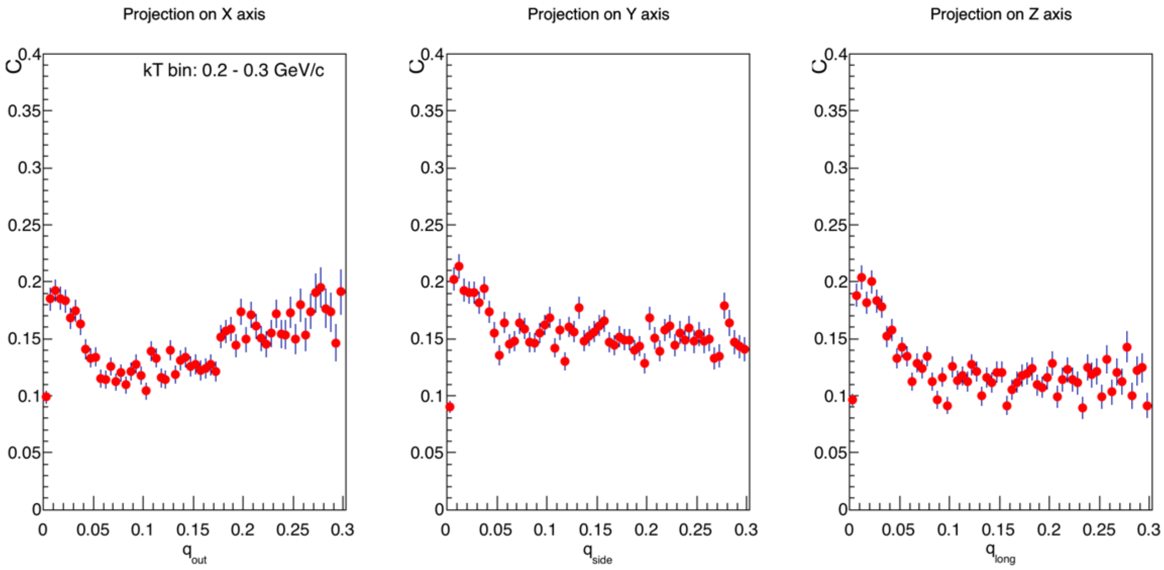

Figure 11: Projections of the correlation function, $k_T = [0.2 - 0.3]$ GeV/c.

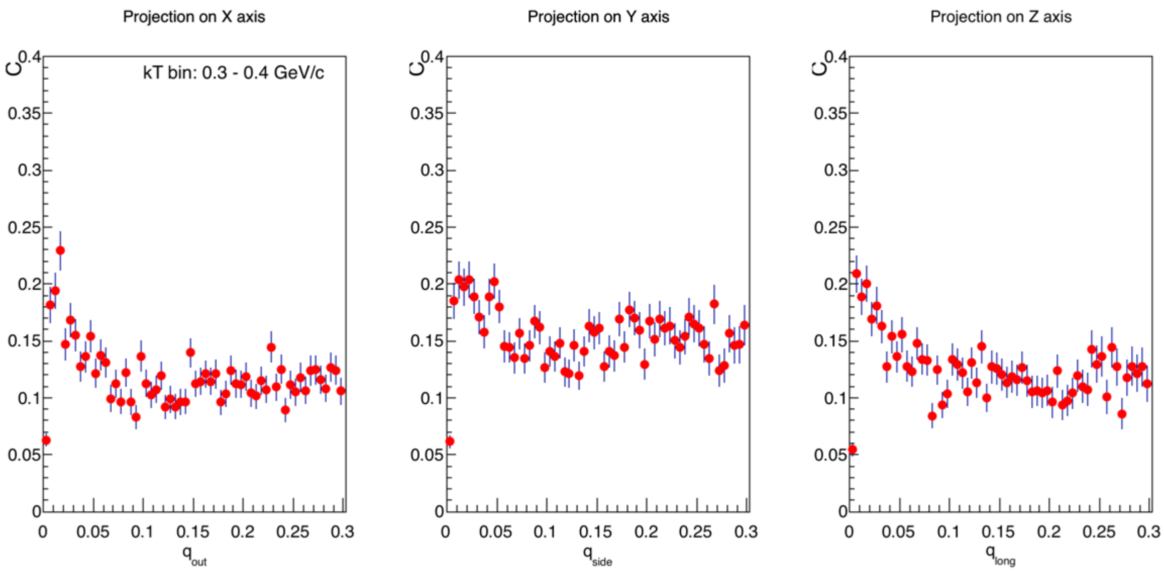

Figure 12: Projections of correlation function, $k_T = [0.3 - 0.4]$ GeV/c.

distribution, denominator). The probability of emission of two particles in the same direction is much smaller than in different ones. This fact reveals itself in a smooth increasing of values of the correlation function with q increasing.

The performed analysis would help in the future work on the data reconstruction and also it gives information on correlations between measured pions.

References

[1] Dabrowski D. et al. Modular and adaptable control system for high energy physics experiments/detectors bm@n and mpd at jinr in dubna. presented on XVII GDRE WORKSHOP Heavy Ions at Relativistic Energies, Nantes, France, 2015.

[2] The nica complex. http://nica.jinr.ru/complex.php. Accessed: 2016-08-28.

[3] H. Zbroszczyk. Studies of baryon-baryon correlations in relativistic nuclear collisions registered at the STAR experiment.

[4] K. Grebieszkow. Lecture: "Introduction to physics of heavy-ion collisions".

[5] Dirk H. Rischke and Miklos Gyulassy. The Time-Dealy Signature of Quark-Gluon-Plasma Formation in Relativistic Nuclear Collisions. 1996.

[6] M. Stefaniak. Examination of heavy-ion collisions with EPOS model in frame of BES program, work in progress.

[7] K. R. Mikhailov, A. V. Stavinsky, A. V. Vlassov, B. O. Kerbikov, and R. Lednicky. Source-size measurements in the $e^3He3(^4He) \to e'p\Lambda X$ reaction. *Phys. Atom. Nucl.*, 72:668–674, 2009.

6 Acknowledgments

I would like to express my gratitude to my supervisors Oleg Rogachevsky, Ludmila Malinina and Pavel Batyuk. Thanks to them I relevantly developed my knowledge in the femtoscopy correlations. I really do appreciate all discussion with Ludmila and Pavel, where they explained me the most difficult and complex problems in my studies.

I would also like to thank organizing committee, especially Elena Karpova, for taking care of all issues connected with my travel to Russia and stay in Dubna. My internship would not be possible without financial support of Joint Institute for Nuclear Research.

The last but not the least, I would like to thank my Polish supervisors Jan Pluta and Hanna Zbroszczyk, who encouraged me to come to Dubna and helped with preparation to this internship.